

Carbon nanotube-based synthetic gecko tapes

Liehui Ge*, Sunny Sethi*, Lijie Ci†, Pulickel M. Ajayan†, and Ali Dhinojwala**

*Department of Polymer Science, University of Akron, Akron, OH 44325-3909; and †Department of Materials Science and Engineering, Rensselaer Polytechnic Institute, Troy, NY 12180-3590

Communicated by Jacob N. Israelachvili, University of California, Santa Barbara, CA, April 17, 2007 (received for review December 7, 2006)

We have developed a synthetic gecko tape by transferring micropatterned carbon nanotube arrays onto flexible polymer tape based on the hierarchical structure found on the foot of a gecko lizard. The gecko tape can support a shear stress (36 N/cm²) nearly four times higher than the gecko foot and sticks to a variety of surfaces, including Teflon. Both the micrometer-size setae (replicated by nanotube bundles) and nanometer-size spatulas (individual nanotubes) are necessary to achieve macroscopic shear adhesion and to translate the weak van der Waals interactions into high shear forces. We have demonstrated for the first time a macroscopic flexible patch that can be used repeatedly with peeling and adhesive properties better than the natural gecko foot. The carbon nanotube-based tape offers an excellent synthetic option as a dry conductive reversible adhesive in microelectronics, robotics, and space applications.

adhesives | nanomaterials | hierarchical | robotics

Flexible adhesive tapes are indispensable in our daily lives, whether it is to leave a note to a friend or to seal packages. However, we rarely hang heavy objects on a wall using these tapes because the stickiness is time- and rate-dependent. The viscoelastic tapes do not work under vacuum, such as space applications, and where repeated attachment and detachment is required, such as wall-climbing robots. Nature has found an alternate solution to stick to surfaces without using sticky viscoelastic liquids. Natural selection has developed the wall-climbing lizard's foot (Fig. 1A) in a hierarchical structure, consisting of microscopic hairs called setae, which further split into hundreds of smaller structures called spatulas (Fig. 1B) (1–4). On coming in contact with any surface, the spatulas deform, enabling molecular contact over large areas, thus translating weak van der Waals interactions into enormous attractive forces (4). There have been several theoretical models to elucidate the mechanism of gecko adhesion (5). However, it is not clear why nature has developed this intricate hierarchical structure of micrometer-size setae and nanometer-size spatulas on the gecko foot, instead of covering the whole feet with only setae or spatulas. Many synthetic structures using uniform polymer pillars and in some cases hierarchical structures (6, 7) have been constructed before, although the performance of these structures has not been as good as natural gecko (8, 9). One limitation of these polymer pillars with a high aspect ratio is that they are mechanically weak in comparison to keratin used in the natural foot-hairs.

Here we have replicated the multiscale structure of setae and spatulas using microfabricated multiwalled carbon nanotubes and found that not only nanometer-length scales of spatulas (individual carbon nanotubes) but also micrometer-length scales of setae (patterns of carbon nanotubes) are important to support large shear forces. Our results show that a 1-cm² area of the carbon nanotube patterns transferred on a flexible tape (referred to as a “gecko tape” hereafter) supports 36 N. These shear forces are a factor of four times higher than the natural gecko foot-hairs, a factor of 10 higher than polymer pillars (8, 9), and a factor of four times higher than unpatterned carbon nanotube patches on silicon (10). Similar shear forces are obtained on both hydrophilic (mica and glass) and hydrophobic (Teflon) surfaces. These synthetic gecko tapes show shear and peeling properties

that are similar to those found on gecko feet and offer an excellent synthetic option as a dry conductive reversible adhesive in microelectronics, robotics (11), and space applications.

Results and Discussion

The natural gecko foot (Fig. 1A) has 25- μ m-diameter setae arranged in many lobes along the foot, and the SEM image in Fig. 1B shows 100- to 200-nm-diameter spatulas (4). The synthetic setae and spatulas fabricated using aligned carbon nanotubes are shown in the SEM images in Fig. 1C–H. Fig. 1C and D shows the picture of carbon nanotubes on a flexible gecko tape to illustrate the similarity in the natural and synthetic hairs. We have also fabricated different sizes of the carbon nanotube patches ranging from 50 to 500 μ m in width (Fig. 1E–H). The synthetic setae consist of thousands of synthetic spatulas, which are individual bundles of aligned carbon nanotubes (average diameter of 8 nm) shown at higher magnification in Fig. 1D. We have chosen carbon nanotubes to construct the synthetic setae because our recent atomic force microscopy results show that the vertically aligned carbon nanotubes have strong nanometer-level adhesion with a silicon tip (12) and have excellent mechanical properties. The synthetic setae were fabricated by using a conventional photolithography patterning process. The catalyst (Fe and Al) was deposited on a silicon substrate as patches with dimensions shown in Fig. 1D–H. The carbon nanotubes were grown at 750°C using a mixture of ethylene and hydrogen gas, and the carbon nanotubes grew only in the areas covered with the catalyst. The length of carbon nanotubes was controlled by the reaction time and was \approx 200–500 μ m for the structures fabricated for this study.

To measure the macroscopic adhesion forces, small areas of flexible gecko tapes were pressed against a smooth mica sheet using a cylindrical roller. This is equivalent to a pressure of 25–50 N/cm² to deform the gecko tape and the carbon nanotube structures to achieve good contact between the tape and the substrate. The actual shear measurements were done under no external normal load as shown in Fig. 2A Inset. We have chosen this geometry to compare these synthetic materials with the force measurements on live geckos that were done by using an almost vertical geometry by Irschick *et al.* (13). This is equivalent to dragging the gecko almost parallel to the surface. The shear force for the unpatterned gecko tape for a 0.16-cm² patch is shown in Fig. 2A. We have compared these shear forces with the force supported by the live geckos calculated in the units of force supported by a 0.16-cm² area (10 N/cm² \times 0.16 cm²). The forces supported by the synthetic structures are comparable to the live gecko measurements. The force supported by 0.12-cm² and 0.25-cm² patch was 1.2 N and 1 N, respectively, and the shear force does not increase with the area of the tape. This is a disadvantage because we cannot scale up the weight supported by the gecko tape by increasing the contact area.

Author contributions: L.G. and S.S. contributed equally to this work; P.M.A. and A.D. designed research; L.G., S.S., and L.C. performed research; L.C. and P.M.A. synthesized the carbon nanotubes; and A.D. wrote the paper.

The authors declare no conflict of interest.

†To whom correspondence should be addressed. E-mail: ali4@uakron.edu.

© 2007 by The National Academy of Sciences of the USA

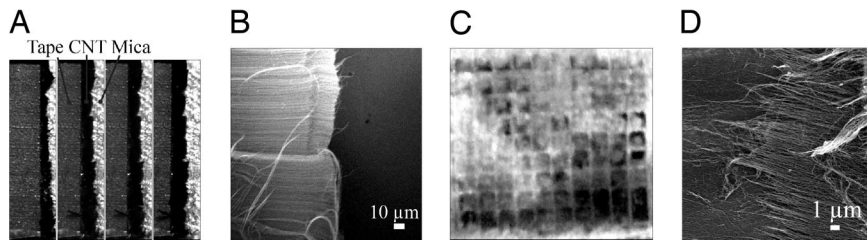


Fig. 3. Optical and SEM images of the carbon nanotubes during loading and after the crack has propagated through the sample. (A) Four optical pictures of the tape (5 mm × 5 mm area) cropped to show only the edges of the tape under different shear loads (20, 70, 140, and 190 g). The black region is the compressed carbon nanotubes sticking out of the edges of the tape and making intimate contact with the substrate. (B) A SEM picture of the edge of tape where we observe the deformation of the carbon nanotubes after it has been pressed in contact with the mica surface. The edge observed in the middle of the SEM picture is the boundary between the carbon nanotubes and the substrate. (C) The optical picture of the mica surface showing the carbon nanotubes left on the mica surface after the crack has propagated. (D) SEM image of the carbon nanotubes left behind on the mica surface.

a certain critical load a catastrophic rupture is initiated; the failure is cohesive, and carbon nanotube residues are left behind on the mica surface (Fig. 3C). No carbon nanotube residue is left behind on the mica substrate when the tapes are peeled at different angles (in a peeling geometry rather than shear geometry), similar to how a gecko walks, and the results are discussed later. This cohesive failure indicates that the interfacial adhesion strength is sufficient to support large shear forces. The 50- to 500- μm patterned surfaces are important in supporting larger shear stress and increasing the total shear force supported by the tape by increasing the contact area (similar force/area values were obtained for gecko tapes of 0.16 cm^2 and 0.25 cm^2 area).

The SEM image of the carbon nanotube residues remaining on the mica surface is shown in Fig. 3D. The aligned and broken strands of the carbon nanotube bundles indicate that there is large energy dissipation in the cohesive failure. In the case of unpatterned gecko tapes, the failure was interfacial with very little carbon nanotube remaining on the mica surface after peeling. The optical and SEM images show that the 50- to 500- μm patches deform and hinder the crack growth. In fracture mechanics it has been demonstrated that the resistance to the propagation of cracks is very important in increasing the toughness of the materials (15). In the case of adhesive tapes, Kendall has shown that the peeling strength of tapes with patches of different stiffness or thickness can be much higher than the tapes with uniform thickness and stiffness (16). Chaudhury and co-workers have shown that 100- to 200- μm patches on poly(dimethylsiloxane) sheets increases the peeling force by a factor of 10–20 in comparison to a unpatterned poly(dimethylsiloxane) sheet (17). We postulate that the mechanism in all of these cases, including the patterned gecko tape, is to stop, deviate, and reinitiate the crack propagation in comparison to materials with uniform properties (also referred to as the Cook–Gordon mechanism) (15). It is interesting to note that the enhancement in shear stress in the case of natural gecko, poly(dimethylsiloxane) patterns, and synthetic gecko tapes are observed for sizes of patterns that are comparable to the thickness or height of the setae.

We have also measured the force required to peel the gecko tapes at different angles as shown in the Fig. 4A. This peeling measurement is important for two reasons. First, the peeling resistance has to be much smaller in comparison to shear forces in mimicking the gecko feet. The gecko moves or gets unstuck from a surface by uncurling its toes. This is necessary because, at those peeling angles, the peeling forces are weak and the gecko can effortlessly move on a vertical surface by using its foot-hairs repeatedly without any damage. Second, the peeling force divided by the width of the tape (F/w) provides us an approach to determine the energy of detachment (G). The 500- μm patterned synthetic tape peels off the mica substrate with an adhesive force/width of only 16 N/m at a 45° angle, 20 N/m at a

30° angle, and 96 N/m at a 10° angle. This peeling process at angles $>10^\circ$ does not involve any breaking or transfer of the carbon nanotube on the substrate, and the synthetic gecko tape can be reused many times without damage. The low peeling forces at a non-zero angle are due to the preexisting crack at the peeling front. A similar effect is also observed if you peel off the viscoelastic tapes from substrates, where the shear forces are much higher than the peeling forces at non-zero angles (18).

We can calculate the energy of detachment (G) using $G = F(1 - \cos\theta)/\text{width}$ (18), where F is the peeling force and θ is the peeling angle. This equation is for peeling angles $\geq 45^\circ$, and the elastic stiffness of the gecko tape is important at lower peeling angles (18). We find that G is 5 J/m 2 on mica at a 45° peeling angle, which is much larger than the thermodynamic work of adhesion. On Teflon substrates, $G = 2.2 \text{ J/m}^2$ at a 45° peeling angle, consistent with the lower surface energy of Teflon in comparison to mica (summarized in Fig. 4B). These values of G for the carbon nanotube tapes are much larger than the poly-(dimethylsiloxane)-based patterned surfaces reported in the literature (17).

Finally, we would like to discuss whether the shear forces supported by the carbon nanotube gecko tapes are due to adhesion or high friction as suggested recently for micrometer-size polypropylene fibers (19). Currently, there are several arguments that support the idea of adhesion playing an important role. First, the shear experiments were done under negligible normal load (just the weight of the tape, $\approx 20 \text{ mg}$). Second, when the tape breaks under load we observe the crack front (by video camera) moving at speeds $>10 \text{ m/s}$, which are expected for adhesive stick to sliding (or breaking) transition. Third, the high nanometer-level pull-off forces were observed by using atomic force microscopy silicon tip in contact with carbon nanotube bundles (12). Fourth, we were also able to support normal loads

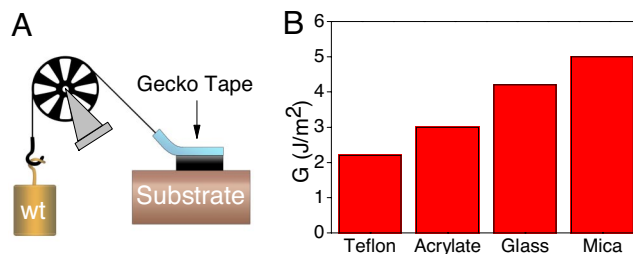


Fig. 4. Peeling measurements of the gecko tapes on various substrates. We performed the peeling measurements at different angles using the setup shown in A. (B) The energy of detachment, G (J/m 2), plotted at a peeling angle of 45° on various substrates.

of 3–5 N/cm² for patterned and unpatterned gecko tapes on mica substrate, which has to result from adhesion rather than friction.⁸

In summary, we have fabricated hierarchical structures of setae and spatulas found on the gecko foot using aligned multiwalled carbon nanotubes. The multiscale structures with length scales of micrometers (setae) and nanometers (spatulas) are necessary to achieve high shear and peeling forces. Using these concepts, we have shown that a 1-cm² area can support nearly 4 kg of weight and that much larger forces can be supported by increasing the area of the tape.

Methods

Procedure to Grow Carbon Nanotubes. The experimental process for the growth of aligned carbon nanotubes involves three steps: photolithography, catalyst deposition, and a chemical vapor deposition process. After the photolithographic pattern process, an electron beam was used to deposit a 10-nm-thick aluminum (Al) buffer layer on a Si or Si/SiO₂ wafer. On top of the Al layer, a 1.5-nm-thick iron catalyst layer (which forms nanosized particles for catalytic growth of carbon nanotubes) was deposited. Chemical vapor deposition set up to grow carbon nanotubes consists of a tubular furnace with an alumina processing tube (inner diameter 45 mm). Aligned carbon nanotube films were prepared by thermal decomposition of ethylene (with a flow rate of 50–150 standard cubic centimeters per minute) on the catalyst film at 750°C. An Ar/H₂ gas mixture (15% H₂) with a flow rate of 1,300 standard cubic centimeters per minute was used as the

buffer gas during the whole chemical vapor deposition run. A very low concentration of water vapor with a dew point of –20°C was carried to the reaction furnace by a fraction of Ar/H₂ flow during carbon nanotube growth (20). The growth time is 10–30 min, and the length of carbon nanotubes is ≈200–500 μm. The average diameter of the carbon nanotubes is 8 nm (two to five walls).

Adhesion Measurements. A freshly cleaved mica surface was prepared by lifting off a thin layer of mica sheet with an adhesive tape. The glass substrate was cleaned in a base bath, followed by rinsing with deionized water. The final washing was done in water containing a small amount of surfactant, which coats the glass with a monolayer of surfactant and prevents any further condensation of impurities from the atmosphere. The glass substrate was plasma-treated for 5 min in oxygen plasma before the adhesion measurements. The poly(methyl methacrylate) and poly(octadecyl acrylate) films were prepared by spin coating a 100- to 200-nm-thick layer on a silicon substrate. The samples were annealed above the glass transition temperature for poly(methyl methacrylate) and above the melting temperature for poly(octadecyl acrylate) polymer under vacuum. The Teflon sample was cleaned for 6 h in a mixture of Nochromix and sulfuric acid. The Teflon sample was rinsed with deionized water and dried under nitrogen. The carbon nanotubes on the silicon substrate were transferred on flexible adhesive tapes (for the force measurements we have used 3M Scotch tapes), and the carbon nanotubes were peeled off the silicon substrate with exposing the ends that were in contact with the silicon substrate (synthetic gecko tape). The synthetic gecko tape was pressed lightly with the substrate by using a cylindrical roller. All measurements were performed at ambient conditions.

⁸These measurements were done by supporting weight perpendicular to the substrate. It was important to do this measurement by keeping the tape and the substrate parallel so that the normal force is applied uniformly across the tape. This was not always possible, and the tape peeled off from the substrate instead. Therefore, the measured numbers may be lower than what can be actually supported by these gecko tapes. Similar low numbers are obtained for viscoelastic adhesive tapes on normal loading.

We acknowledge financial support from National Science Foundation Division of Materials Research Grant 0512156 and Nanoscale Interdisciplinary Research Teams Grant 0609077.

1. Gorb S (2001) *Attachment Devices of Insect Cuticle* (Kluwer Academic, Dordrecht, The Netherlands).
2. Arzt E, Gorb S, Spolenak R (2003) *Proc Natl Acad Sci USA* 100:10603–10606.
3. Autumn K, Liang YA, Hsieh ST, Zesch W, Chan WP, Kenny TW, Fearing R, Full RJ (2000) *Nature* 405:681–685.
4. Autumn K, Sitti M, Liang YA, Peattie AM, Hansen WR, Sponberg S, Kenny TW, Fearing R, Israealachvili JN, Full RJ (2002) *Proc Natl Acad Sci USA* 99:12252–12256.
5. Gao H, Wang X, Yao H, Gorb S, Arzt E (2005) *Mech Mater* 37:275–285.
6. Northen MT, Turner KL (2006) *Sensors Actuators A* 130–131:583–587.
7. Northen MT, Turner KL (2005) *Nanotechnology* 16:1159–1166.
8. Geim AK, Dubonos SV, Grigorieva IV, Novoselov KS, Zhukov AA, Shapovalov SY (2003) *Nat Mater* 2:461–463.
9. Sitti M, Fearing RS (2003) *J Adhes Sci Technol* 17:1055–1073.
10. Zhao Y, Tong T, Delzeit L, Kashani A, Meyyappan M, Majumdar A (2006) *J Vac Sci Technol B* 24:331–335.
11. Daltorio KA, Horschler AD, Gorb S, Ritzmann RE, Quinn RD (2005) in *Proceedings of the International Conference on Intelligent Robots and Systems* (Inst of Electrical and Electronics Engineers, New York), pp 3648–3653.
12. Yurdumakan B, Raravikar NR, Ajayan PM, Dhinojwala A (2005) *Chem Commun*, 3799–3801.
13. Irschick DJ, Austin CC, Ken P, Fisher RN, Losos JB, Ellers O (1996) *Biol J Linn Soc* 59:21–35.
14. Huber G, Mantz H, Spolenak R, Mecke K, Jacobs K, Gorb SN, Arzt E (2005) *Proc Natl Acad Sci USA* 102:16293–16296.
15. Gordon JE (1984) *The New Science of Strong Materials, or Why You Don't Fall Through the Floor* (Princeton Univ Press, Princeton), 2nd Ed.
16. Kendall K (1975) *Proc R Soc Lond Ser A* 341:409–428.
17. Chung JY, Chaudhury MK (2005) *J R Soc Interface* 2:55–61.
18. Gent AN, Kaang SY (1987) *J Adhes* 24:173–181.
19. Majidi C, Groff RE, Maeno Y, Schubert B, Baek S, Bush B, Maboudian R, Gravish N, Wilkinson M, Autumn K, et al. (2006) *Phys Rev Lett* 97:076103.
20. Hata K, Futaba DN, Mizuno K, Namai T, Yumura M, Iijima S (2004) *Science* 306:1362–1364.